
Act in Collusion: A Persistent Distributed Multi-Target Backdoor in Federated Learning

Tao Liu, Wu Yang,* Chen Xu, Jiguang Lv, Huanran Wang,
Yuhang Zhang, Shuchun Xu, Dapeng Man
College of Computer Science and Technology
Harbin Engineering University
Harbin, 150001

{liutaojisuanji, yangwu, chen.xu, mandapeng}@hrbeu.edu.cn

Abstract

Federated learning, a novel paradigm designed to protect data privacy, is vulnerable to backdoor attacks due to its distributed nature. Current research often designs attacks based on a single attacker with a single backdoor, overlooking more realistic and complex threats in federated learning. We propose a more practical threat model for federated learning: the distributed multi-target backdoor. In this model, multiple attackers control different clients, embedding various triggers and targeting different classes, collaboratively implanting backdoors into the global model via central aggregation. Empirical validation shows that existing methods struggle to maintain the effectiveness of multiple backdoors in the global model. Our key insight is that similar backdoor triggers cause parameter conflicts and injecting new backdoors disrupts gradient directions, significantly weakening some backdoors performance. To solve this, we propose a **Distributed Multi-Target Backdoor Attack** (DMBA), ensuring efficiency and persistence of backdoors from different malicious clients. To avoid parameter conflicts, we design a multi-channel dispersed frequency trigger strategy to maximize trigger differences. To mitigate gradient interference, we introduce *backdoor replay* in local training to neutralize conflicting gradients. Extensive validation shows that 30 rounds after the attack, Attack Success Rates of three different backdoors from various clients remain above 93%.

1 Introduction

Federated Learning (FL) [19, 31, 56] enables decentralized devices to collaboratively train a global model without data sharing, enhancing privacy and reducing transmission costs. This approach uses a central server to aggregate updates from client nodes, each with its own dataset, and is promising in sectors like finance, healthcare, and autonomous driving [28, 41, 6]. However, FL's distributed nature introduces significant security challenges [53, 60, 45, 4], notably backdoor attacks [13, 38, 36] that stealthily misclassify specific triggers without impacting the main task performance. Secure aggregation [42] facilitates backdoor attacks by limiting server access to client updates, emphasizing the need for focused research in federated learning.

Existing backdoor attacks are classified into *single-target* [53, 13, 38, 36, 7, 2, 29] and *multi-targets* [23, 21, 54, 3, 55, 16] based on the number of target labels. Single-target attacks have one misclassification task, misclassifying inputs that meet specific triggers into a predetermined class during inference. Multi-target attacks involve multiple labels, activating different backdoors for various triggers to perform targeted misclassifications. However, these models don't fit the complex attack scenarios in FL, where multiple attackers may control different clients, each with unique triggers and target labels, and launch attacks at different times. Single-target

*Corresponding author.

models assume a single backdoor type, while multi-target models rely on centralized computing, both unsuitable for FL’s decentralized nature. Consequently, there is a gap in research regarding complex FL attack scenarios and the effectiveness of backdoor attacks in such settings.

Additionally, we empirically validated the limitations of existing backdoor methods, which struggle in complex scenarios to maintain high Attack Success Rates (ASRs) for multiple backdoors, as demonstrated in Fig. 1 (details in Appendix A). The underperformance stems from two main issues: high similarity among backdoor triggers causing severe model parameter conflicts and the injection of new backdoor samples producing conflicting gradients with previous samples [2], which diminish the impact of past malicious updates.

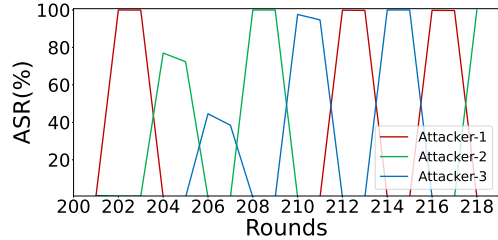


Figure 1: ASRs for multiple backdoors in complex attack scenarios.

To address complex attack scenarios in federated learning, we introduce a new backdoor attack, DMBA, noted for its efficiency and durability. We begin by analyzing the characteristics of attack scenarios in FL and propose a new threat model. Next, we develop a multi-target trigger strategy to activate backdoors efficiently and covertly, avoiding parameter conflicts. Lastly, we introduce a backdoor replay component for local training to mitigate gradient interference during model aggregation. Extensive validation confirms DMBA maintains high ASR, with averages over 93% across tasks and above 83% after 30 rounds.

Our contributions are summarized as follows:

- We introduce DMBA, a distributed multi-target backdoor attack in federated learning, characterized by its practical threat model and new objective function tailored for complex scenarios. DMBA outperforms three baseline attacks in terms of persistence and stealth across various datasets and models. We also evaluated the impact of the *backdoor replay* component and several important factors on DMBA performance through ablation studies and a series of hyperparametric sensitivity analyses. Finally, we evaluated DMBA under two state-of-the-art defenses, demonstrating its strong robustness.
- We develop a trigger strategy based on multi-channel dispersed frequency block perturbations. This strategy addresses the performance decline caused by high similarity among backdoor triggers, which leads to parameter conflicts in the global model. By transforming pixel matrices of different channels into the frequency domain and perturbing different frequency blocks, this approach enhances trigger distinguishability while maintaining stealth.
- We propose a backdoor replay component, inspired by the idea of experience replay, to guide the backdoor training process in malicious clients. This component allows learning from a small amount of previous backdoor samples alongside new ones, neutralizing conflicting gradients and extending the poisoning duration, thereby mitigating catastrophic forgetting in backdoors.

2 Related Work

Backdoor attacks in FL. In FL backdoor attacks, attackers inject malicious updates into client models, aiming to compromise the aggregated global model. Bagdasaryan et al. [2] first introduced such attacks in FL, using amplified malicious updates to enhance the backdoor’s effect. Bhagoji et al. [5] improved attack efficiency by increasing the local learning rate before convergence and introduced stealth through an alternating minimization strategy. Xie et al. [53] pioneered distributed backdoor attacks, leveraging FL’s nature to aggregate multiple locally trained triggers, enhancing stealth and efficiency. Liu et al. [29] addressed the decay in backdoor attack success over rounds with a combinatorial distributed trigger strategy, boosting attack persistence. **However**, these approaches primarily assume single-target attacks, which oversimplify the diverse and complex scenarios in FL with multiple potential attackers and targets. Our work addresses this gap by focusing on realistic, multi-target attack scenarios in FL.

Multi-target backdoor attacks. Multi-target backdoor attacks feature multiple backdoors each with unique target labels, activated under specific triggers to perform diverse tasks within a compromised model. Pioneering efforts like Hyun et al. [23, 21] used fixed and location-variable triggers requiring separate model trainings, not fully conforming to standard multi-target attacks. Others, like Xue et al. [54], utilized varying intensities of the same trigger pattern, while Barni et al. [3] employed clean-label tactics with different signals for diverse backdoors. More advanced approaches like those of Xue et al. [55], employing steganography, and Hou et al. [16], using semantic triggers from clean samples, aimed to increase stealth and ambiguity. **A major limitation** of these methods is their dependence on centralized computing paradigms, as they require access to all user data, restricting their practicality. A recent research [46] indicates that multi-target attacks are only feasible in centralized setups where injections occur simultaneously—unrealistic in typical FL settings. Our DMBA model addresses this by excelling in distributed attack scenarios, thus bypassing traditional centralized constraints.

Backdoor defenses in FL. In FL, backdoor defenses are categorized based on their operational phase: *previous-aggregation defense* (Pre-AD), *in-aggregation defense* (In-AD), and *post-aggregation defense* (Post-AD). Pre-AD methods, like FoolsGold [10] and FLDetector [59], identify and exclude malicious clients by analyzing update anomalies before aggregation. In-AD strategies, such as differential privacy [11], DP-FedAvg [32] and ClippedClustering [25], employ robust techniques like parameter clipping and noise addition during aggregation to mitigate backdoor effects. Post-AD methods, exemplified by Pruning Neurons [51] and KD Unlearning [52], modify the global model after aggregation to remove harmful updates and "forget" backdoor effects, maintaining task performance. Pre-AD methods require analysis of all client updates, which can conflict with FL’s privacy-preserving principles, making them challenging to deploy in practical FL scenarios, especially when high data variability leads to inaccurate detection of malicious updates. Post-AD methods are less efficient as they allow the poisoned model to impact outcomes before corrective actions are taken, potentially leading to persistent backdoors or loss of benign learning. In contrast, **In-AD methods are considered the most reasonable for backdoor defense in FL**, though they are mostly validated against single-target backdoor models, **with their effectiveness in more complex attack scenarios yet unproven**. We demonstrate DMBA’s robustness against two In-AD methods in Section 4.6.

3 Methodology

3.1 New Threat Model

A complex attack scenario in FL. In FL, real-world attack scenarios are complex, involving multiple attackers who control distinct clients, each with unique backdoor tasks defined by different triggers or target labels. These backdoors can also be injected into the model at different times. To simulate such complexity, we employ a *distributed collusive attack* model within an FL-based image classification system [30]. In this setup, attackers poison their local training data [44] with unique backdoors and embed them into their local models. Through model replacement techniques [2], they amplify their malicious updates to enhance the performance of each backdoor in the global model, allowing for the sequential and coexistent injection of diverse backdoors.

Attackers’ goal. From the client’s perspective, each attacker aims to inject a unique backdoor into their local model that functions effectively without affecting the model’s primary task, as shown in Eq. 1. Here, n represents the total number of attackers, l denotes the cross-entropy loss, y_i is the true label of sample x_i , τ_n is the target label for the n -th attacker, and b signifies the backdoor operation, which involves adding the trigger ϕ_n to sample $x_{i'}$. From the server’s perspective, the unified goal is to inject these backdoors into the global model through aggregation, ensuring they are effective, persistent, and coexist without compromising the model’s overall accuracy, detailed in Eq. 2. Here, y^{cln} is the true label of x_i^{cln} , while $b(x_{i'}^{poi}; \phi_n)$ and τ_n correspond to the backdoored sample and target label of the n -th attacker, respectively. This shared objective classifies DMBA as a collusive attack [1]. Effectiveness of a backdoor is determined if the global model classifies any input with one of the designated triggers as the corresponding target class. Given the continuous updates in FL and the impracticality of attackers updating endlessly [60, 40], it’s crucial to focus on the ASRs within

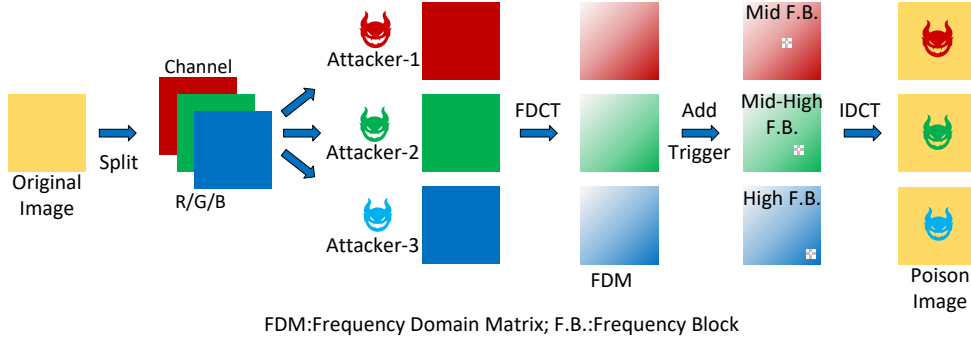


Figure 2: **Distributed multi-target trigger strategy.** Different attackers convert pixel matrices of various channels into the frequency domain and then perturb different frequency blocks to serve as triggers, activating backdoors with distinct target labels.

limited communication rounds.

$$\theta_n^* = \arg_{\theta_n} \min \left(\sum_{x_i \in D_n^{cln}} l[f(x_i; \theta_n), y_i] + \sum_{x_{i'} \in D_n^{poi}} l[f(b(x_{i'}; \phi_n); \theta_n), \tau_n] \right) \quad (1)$$

$$\theta_{GM}^* = \arg_{\theta_{GM}} \min \left(\sum_i l[f(x_i^{cln}; \theta_{GM}), y^{cln}] + \sum_n \sum_{i'} l[f(b(x_{i'}^{poi}; \phi_n); \theta_{GM}), \tau_n] \right) \quad (2)$$

Attackers' knowledge and capability. Following Kerckhoffs' principle [39], we use assumptions similar to those in DBA [53] and FCBA [29]. Each attacker targeting a unique backdoor has full control over their client's training process, including managing local data, updating models, and fine-tuning hyperparameters during iterations. This setup doesn't impact other participants or the central server, making it practical for FL environments.

3.2 Distributed Multi-Target Trigger

To maximize stealth in backdoor attacks, triggers should be nearly invisible. Frequency domain triggers [55, 47, 57, 9], particularly effective due to their subtlety, convert images from the spatial to the frequency domain. Minimal changes in this domain can activate backdoors with high probability while remaining undetectable by the human eye. We use **Discrete Cosine Transform** (DCT)-based frequency domain triggers [47] for activating DMBA, given their excellent energy compression and minimal visual artifacts.

Our distributed multi-target trigger strategy, depicted in Fig. 2 for three attackers ($n=3$), involves each attacker selecting a different color channel (R/G/B) and applying DCT to convert these channels into the frequency domain. Slight perturbations are introduced at various frequency blocks as triggers. The altered frequency matrices are then reverted to pixel space, and image labels are updated to the attackers' specified target labels, creating distinct backdoor samples. We focus on perturbing mid to high frequency bands to avoid significant visual quality loss that low frequency alterations would cause. This strategy and the corresponding backdoor attack are applicable for $n \geq 2$, detailed in Appendix B. Tab. 5 shows the specific trigger strategies for $n=3$ and $n=6$, while Tab. 6 demonstrates that DMBA still performs well with six backdoors, maintaining an average ASR over 95% and above 90% after 30 rounds.

Our trigger strategy is informed by prior research [47, 46] and extensive testing, which showed that similar triggers across different backdoors can cause model parameter conflicts and degrade performance. To counter this, we chose different pixel channels and introduced perturbations in various frequency blocks to activate unique backdoors, effectively preventing overlap in trigger patterns. As demonstrated in Tab. 3, baseline attacks lacking this careful design face severe parameter conflicts in distributed multi-target settings, significantly lowering the ASR of some backdoors.

3.3 Backdoor Replay Component

Our review of prior studies [2, 53, 29] and experiments show that catastrophic forgetting [24] and gradient direction interference significantly impact the performance of DMBA in federated learning. Studies by Xie et al. [53] and Liu et al. [29] highlight that federated learning’s multitasking nature [18, 8, 27] leads to catastrophic forgetting of backdoors when injections stop and the model focuses on primary tasks, diluting the backdoor’s effectiveness with benign updates [34, 12]. Furthermore, introducing a new backdoor sharply decreases the ASR of previously injected backdoors due to gradient direction interference [2], as new conflicting gradients can negate earlier malicious updates, significantly reducing their effectiveness, shown in Tab. 4 where ASRs nearly drop to zero during new injection rounds.

Inspired by the classic DQN approach [33, 37, 15] in reinforcement learning, we developed a **Backdoor Replay** component for malicious clients in FL. This module, by guiding local backdoor training, significantly reduces the impacts of catastrophic forgetting and gradient direction interference, thus enhancing DMBA’s persistence. Backdoor Replay involves including small quantities of different backdoor samples during single backdoor training rounds to improve all backdoors’ performance. This approach spreads each backdoor across more rounds over a wider timeline without extra costs, mitigating ASR decay from forgetting. It also neutralizes conflicting gradients, softening the negative effects of update offset on ASR. The creation of the Backdoor Replay component follows two steps: (1) **Build a backdoor replay pool**. As described in Section 3.1, before selecting their clients, attackers gather network data to create backdoor samples for replay, denoted as D_{br_n} for the n -th attacker. These are combined into the backdoor replay pool $Pool_{br}$, held by each attacker, where $Pool_{br} = \Sigma D_{br_n}$. (2) **Share the replay pool and replay backdoor samples**. Once attackers control their clients, $Pool_{br}$ is added to the local training data. During normal training rounds, $Pool_{br}$ isn’t used, but in backdoor injection rounds, a few samples from $Pool_{br}$ are selected for replay in that batch, ensuring these have different targets from the current backdoor. For illustration, the local data composition for training involving three attackers is shown in Eq. 3 (detailed derivation in Appendix C).

$$D_{b_n} = D_{poi_1} + D_{poi_2} + D_{poi_3} + D_{cln}, \quad n = 1, 2, 3 \quad (3)$$

where D_{b_n} represents the dataset used by attacker n for training. D_{cln} is clean data, while $D_{poi_1,2,3}$ refer to three types of backdoor samples: one created by the current attacker and two sourced from $Pool_{br}$. Similarly, the composition of the attacker’s poisoned batch is specified in Eq. 4, where the quantity of each sample type is calculated using Eq. 5. Specifically, bs_{poi_i} are the backdoor samples created by the current attacker, $bs_{poi_j,k}$ are the replayed samples, r_b and r_{br} denote the ratios of backdoor poisoning and replay within the batch, respectively. The rest are clean samples.

$$bs_n = bs_{poi_1} + bs_{poi_2} + bs_{poi_3} + bs_{cln}, \quad n = 1, 2, 3 \quad (4)$$

$$\begin{cases} bs_{poi_i} = r_b \cdot bs_n, & i = n \\ bs_{poi_j} = r_{br} \cdot bs_n, & j \neq i \\ bs_{poi_k} = r_{br} \cdot bs_n, & k \neq i, j \\ bs_{cln} = bs_n - bs_{poi_i} - bs_{poi_j} - bs_{poi_k} \end{cases} \quad (5)$$

3.4 Workflow of DMBA

We outline the DMBA workflow, designed for *distributed collusive attacks* in FL, in Fig. 3:

Step1: Multi-target trigger generation. After selecting their controlled clients, attackers poison local samples by designing unique, highly effective, and stealthy triggers based on Section 3.2. These triggers are embedded into some training samples, changing their labels to desired target labels.

Step2: Local backdoor training. Local models are trained using the poisoned samples from **Step 1**, embedding each specific backdoor. Utilizing the **Backdoor Replay** component introduced in Section 3.3, other backdoors’ replay samples are mixed into the poisoned batches to guide the backdoor training process. Training involves lower learning rates and more iterations to enhance backdoor performance within local models.

Step3: Global model poisoning. Following Bagdasaryan et al.’s approach [2], after training, malicious updates are amplified and included in central aggregation to boost backdoor effectiveness.

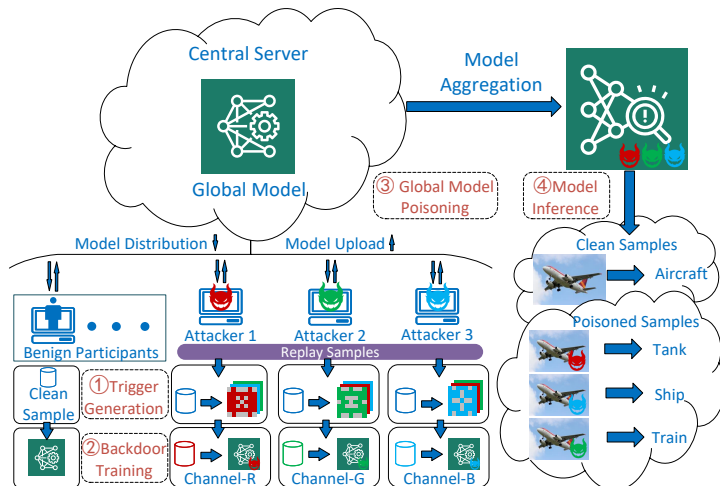


Figure 3: **Workflow of DMBA.** (1)Multi-target trigger generation; (2)Local backdoor training; (3)Global model poisoning; (4)Backdoored global model inference.

Table 1: Datasets and other settings.

Datasets	CIFAR-10	CIFAR-100	GTSRB
Training/Test	50000/10000	50000/10000	39209/12569
Models	(Lw)Resnet-18	Resnet-18	4Conv+2fc
Labels	10	100	43
Input Size	32*32*3	32*32*3	32*32*3
Target labels	#0, #4, #6	#10, #47, #59	#0, #20, #29
Clean ACC	77%	72%	99%

Table 2: Backdoor samples displayment.

clean	DMBA	Bad-t	DMM	Tar-1	
	Att1				
	Att2				
	Att3				

Step4: Backdoored global model inference. The global model, now containing multiple backdoors, operates normally on clean samples but executes designated backdoor tasks on trigger samples, leading to targeted misclassifications.

4 Experiments & Analyses

4.1 Experiment Settings

General setup. Our experiments use a server with 4 NVIDIA A100 GPUs and PyTorch [35] as the software framework. We evaluated our approach across three datasets [20, 43] and models [14], detailed in Tab. 1. (*Lw*) indicates a lightweight model, and *Clean ACC* refers to the performance of the global model on these datasets after convergence, without backdoor insertions.

Multi-object triggers setup. Three attackers (referred to as **Att1**, **Att2** and **Att3**) embed triggers into the R/G/B channels respectively, and perturb a 3*3 frequency block in the DCT-transformed matrices at positions (15, 15), (20, 20), and (25, 25) with a perturbation of +100. Then, they convert these matrices back to pixel matrices using IDCT. Detailed trigger strategy is in Tab. 5 of the Appendix B.

FL & backdoor replay setup. The server uses a learning rate of 0.01 with the FedAvg [31] aggregation algorithm. Locally, training is conducted using stochastic gradient descent [19] with a learning rate of 0.01, momentum of 0.9, decay rate of 0.0005, and the loss is calculated using cross-entropy [2], with a batch size of 64. Benign users perform 2 epochs per local iteration, whereas attackers train for 6 epochs with a lower initial learning rate of 0.05, decaying by a rate of 0.1 per iteration to enhance backdoor persistence. All three datasets utilize a Dirichlet distribution to

approximate non-I.I.D. data distribution in FL, with α set at 0.8. For simplicity, we randomize the order of attacker injections, spacing them one round apart; the first attacker injects at round 202 (i.e. after the model has converged), with each backdoor injected over 3 rounds for effectiveness.

To simplify experiments and maintain attack efficacy, we use a **direct method** for backdoor replay. During backdoor injection rounds, attackers randomly select $2r_{br} \cdot bs_n$ clean images from the current batch and convert each $r_{br} \cdot bs_n$ of these images into one of the other two types of backdoor samples, effectively replaying them. This approach achieves similar backdoor sample counts as those from a pre-built replay pool, simplifying the process without compromising attack performance. Comparisons in Tab. 7 of Appendix D confirm the equivalence of this method.

Evaluation metrics. The evaluation metrics are categorized into two aspects: *attack performance metrics* and *trigger stealth metrics*. The former includes ACC, ASR, and ASR-30, and the latter includes SSIM, LPIPS, and PSNR. These evaluation metrics are summarised below.

ACC \uparrow [17]: The model’s classification success rate on clean samples.

ASR_n \uparrow [26]: The proportion of test samples containing the n -th attacker-specified trigger that are misclassified into the corresponding target class.

ASR_{n-30} \uparrow : ASR for the n -th backdoor, assessed 30 epochs after a DMBA, indicating attack persistence.

SSIM \uparrow [50]: *Structural Similarity Index* measures the perceptual difference between two images, considering changes in structural information.

LPIPS \downarrow [58]: *Learned Perceptual Image Patch Similarity* quantifies image similarity using deep neural networks, emphasizing perceptual relevance.

PSNR \uparrow [49]: *Peak Signal-to-Noise Ratio* evaluates image quality by comparing the peak signal level to the noise level, focusing on pixel-wise accuracy.

4.2 ASR and Attack Persistence of DMBA

We adapted three common trigger strategies to fit distributed multi-target backdoor attacks due to the scarcity of previous work, preserving the original settings as much as possible:

BadNets-t: Based on the patch trigger from BadNets [13], we place four 5*5 white patches at the corners of the original image, activating different backdoors in malicious clients at varying transparencies (20%, 50%, 80%).

DMM: Inspired by Wang et al.’s mask matrix triggers [48], unique mask matrices are embedded in different channels (R/G/B) to activate distinct backdoors.

TargetNet-l: Modifying Kwon et al.’s trigger [22] from squares to triangles to avoid obscuring the central main target, and positioning them at different locations (top-left, bottom-left, top-right) to activate various backdoors.

To ensure robustness and reproducibility, we conducted three experiments and averaged the results, presented in Tab. 3. DMBA consistently achieved high performance, with backdoors’ average ASR exceeding 93%. In contrast, BadNets-t and DMM occasionally experienced backdoor failures. DMBA maintained good attack persistence with an average ASR of over 83% even 30 rounds after the attack. While DMBA minimally impacted main task accuracy, there was a slight decrease on CIFAR-100 due to increased class complexity and challenges in training optimization, which can lead to model capacity issues and overfitting. Fewer samples per class also enhanced the backdoor’s disruption of the main task.

While TargetNet-l matches DMBA in attack performance, it lacks visual stealth. As indicated in Tab. 2, TargetNet-l’s backdoor samples have noticeable visual differences from clean samples, making them easily detectable. In contrast, DMBA’s backdoor samples are visually indistinguishable, enhancing DMBA’s overall effectiveness and stealth.

4.3 Invisibility Assessment

Fig. 4 compares SSIM, LPIPS, and PSNR values across different attack methods, showing that DMBA’s triggers are more invisible than those in baseline methods. Sample demonstrations in Tab. 2 reveal minimal visual differences between DMBA’s backdoor and clean samples, making them nearly imperceptible to the human eye. Overall, DMBA’s trigger strategy provides strong stealth, effectively balancing attack efficiency and stealth as discussed in Section 4.2. Due to space limitations, this

Table 3: Comparing attack performances of different attacks on CIFAR-10, CIFAR-100 and GTSRB.

Datasets	CIFAR-10			CIFAR-100			GTSRB						
Methods	DMBA	BadNets-t	DMM	TargetNet-1	DMBA	BadNets-t	DMM	TargetNet-1	DMBA	BadNets-t	DMM	TargetNet-1	
Acc	72.97%	71.86%	71.02%	73.16%	53.74%	55.83%	52.47%	56.32%	97.72%	98.11%	99.47%	98.33%	
ASR	Att1	96.73%	81.57%	88.63%	96.32%	86.68%	93.26%	80.88%	99.83%	94.51%	3.37%	65.72%	99.36%
	Att2	93.97%	84.17%	97.10%	95.37%	96.19%	94.57%	91.08%	99.67%	91.76%	100%	96.63%	95.41%
	Att3	97.06%	91.06%	95.69%	92.83%	80.42%	99.29%	23.65%	99.04%	95.09%	91.73%	92.30%	89.31%
ASR-30	Att1	73.12%	28.08%	60.98%	87.09%	71.40%	59.39%	65.72%	99.36%	93.14%	89.92%	86.47%	84.63%
	Att2	88.84%	74.73%	90.53%	91.51%	84.45%	82.47%	75.82%	93.24%	99.67%	99.97%	88.71%	92.78%
	Att3	95.99%	92.43%	83.92%	87.39%	67.76%	98.40%	19.77%	98.97%	78.07%	51.18%	88.05%	86.59%

Table 4: Comparison of DMBA attack performance with and without backdoor replay on CIFAR-10, CIFAR-100 and GTSRB.

Datasets	CIFAR-10		CIFAR-100		GTSRB		
	backdoor replay	without backdoor replay	backdoor replay	without backdoor replay	backdoor replay	without backdoor replay	
Acc	73.30%	69.38%	52.63%	45.01%	98.13%	94.70%	
ASR	Att1	96.91%	7.30%	91.19%	0%	98.72%	0%
	Att2	94.49%	99.98%	95.80%	99.96%	99.83%	99.96%
	Att3	99.28%	3.58%	92.25%	0%	99.30%	0%
ASR-30	Att1	78.42%	3.82%	69.07%	0%	96.79%	0%
	Att2	89.34%	94.99%	87.96%	97.30%	99.67%	97.22%
	Att3	97.01%	38.88%	58.71%	0%	99.25%	0%

section only presents the evaluation of trigger invisibility on CIFAR-10. Results for other datasets can be found in Tab. 8 of Appendix E.

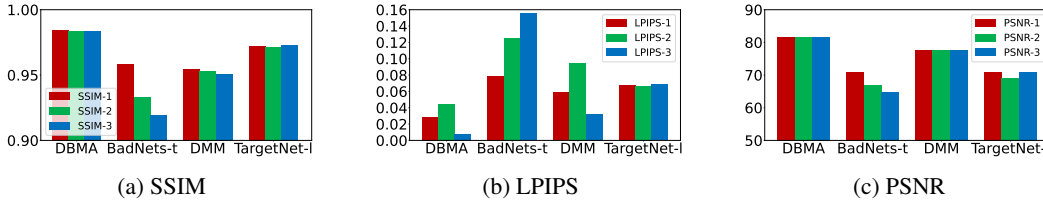


Figure 4: Comparing stealth performances of different attacks on CIFAR-10.

4.4 Ablation Studies

We studied the impact of the Backdoor Replay component on DMBA’s attack performance through controlled experiments: 1) **Experimental Group (with Backdoor Replay)**: Adheres to baseline settings from Section 4.2, with each poisoned batch containing 8 attacker-created backdoor samples, 3 samples each from two replay types, and 50 clean samples. 2) **Control Group (without Backdoor Replay)**: Each poisoned batch consists of 14 attacker-created backdoor samples and 50 clean samples.

Tab. 4 shows that Backdoor Replay significantly boosts DMBA’s performance. In the control group, DMBA generally maintains only the last injected backdoor effectively, with others failing. Conversely, in the experimental group, DMBA sustains an average ASR of 98% for all three backdoors 30 rounds after the attack, demonstrating that Backdoor Replay greatly reduces conflicts between backdoors and ensures their efficiency and persistence.

4.5 Hyperparameter Sensitivity Analyses

In this section, we discuss three key factors affecting DMBA’s performance, with additional factors detailed in Appendix F.

Impact of frequency block starting position f . Each attacker perturbs a 3*3 frequency block in the frequency domain matrices of the R/G/B channel. The optimal starting position combination

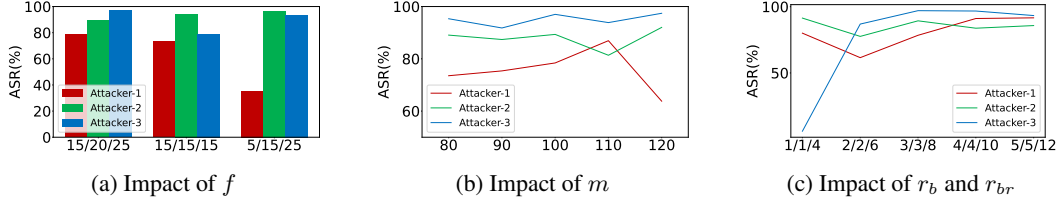


Figure 5: Impact of three key factors on DMBA attack performance on CIFAR-10. The three key factors are: (a) Frequency block starting position; (b) Perturbation magnitude; (c) Poisoning ratio and backdoor replay ratio.

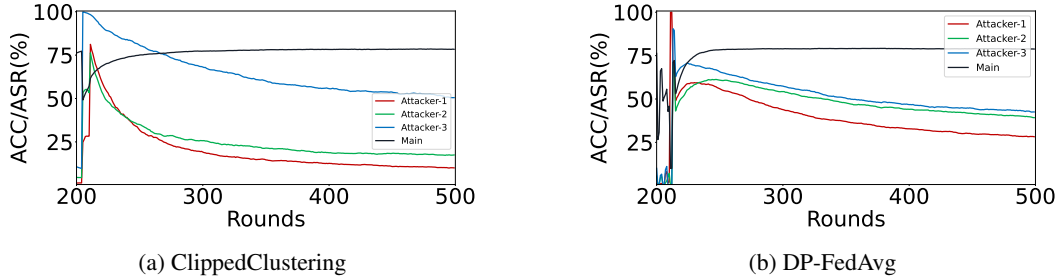


Figure 6: Performance of DMBA on different defence methods on CIFAR-10.

"15/20/25" for these blocks, as shown in Fig. 5a, resulted in the best attack performance. Disturbing higher frequency areas minimally impacts the image, reducing conflicts between backdoors. Spacing out the frequency of disturbances among attackers helps further minimize these conflicts.

Impact of perturbation magnitude m . The magnitude of disturbance within each frequency block also affects attack performance. As demonstrated in Fig. 5b), higher perturbation magnitudes increase the effectiveness of the backdoor attack but also raise the risk of detection due to increased visibility.

Impact of poisoning ratio r_b and backdoor replay ratio r_{br} . Higher poisoning and backdoor replay ratios enhance backdoor performance, as illustrated in Fig. 5c, but may degrade the primary task’s performance. Additionally, incorporating more backdoor samples increases the proportion of anomalies in the local training set, making it easier for detection mechanisms to spot unusual patterns.

4.6 Robustness of DMBA against Defenses

This section evaluates DMBA’s resistance against two advanced In-AD backdoor defense methods mentioned in related works: ClippedClustering and DP-FedAvg. As shown in Fig. 6, despite these defenses, some backdoors in DMBA continue to exhibit significant persistence. Even after 100 rounds post-attack, the strongest backdoor maintains an ASR above 50%. This demonstrates that current defense methods cannot completely neutralize DMBA, highlighting its robustness. Due to space constraints, this section only displays the robustness of DMBA on CIFAR-10. Results for other datasets are provided in Tab. 17 of Appendix G.

5 Conclusion and Future Work

In this paper, we present DMBA, a persistent and stealthy backdoor attack for complex scenarios in FL. DMBA utilizes a multi-channel frequency block perturbation trigger and a backdoor replay component, ensuring multiple backdoors from different clients remain effective in the global model. Our extensive evaluations show that DMBA outperforms existing methods in distributed attack scenarios with multiple attackers. Future work will explore distributed multi-target backdoor attacks for other FL types, such as vertical federated learning and federated transfer learning, and develop defenses against DMBA.

Limitations and Ethical Statements

DMBA faces limitations when applied to scenarios with too many attackers. Our findings indicate that as the number of attackers increases, some backdoors underperform due to the limited capacity of the training models, a common issue in backdoor attacks. This problem, exacerbated by complex or numerous tasks, can be mitigated by using more robust models. Additionally, excessive backdoors can cause trigger similarity and parameter conflicts, causing some backdoors to fail.

The research presented in this paper focuses on identifying potential vulnerabilities in federated learning systems to enhance their security and robustness. While we explore a novel backdoor attack method, our primary intent is to promote awareness and stimulate further research into defensive measures. We acknowledge the potential misuse of such attack techniques; therefore, we have taken several steps to mitigate these risks:

- **Disclosure:** We have responsibly disclosed our findings to relevant stakeholders and developers of federated learning systems to facilitate timely remediation and enhancement of security protocols.
- **Ethical Use:** Our research is conducted under ethical guidelines with the sole purpose of improving the security of machine learning models. We strongly discourage and condemn any malicious use of the techniques discussed.

By highlighting these vulnerabilities, we aim to contribute to the development of more secure and trustworthy federated learning frameworks, ultimately benefiting the broader AI community and society as a whole.

References

- [1] Alharbi, S., Guo, Y., and Yu, W. (2024). Collusive backdoor attacks in federated learning frameworks for iot systems. *IEEE Internet of Things Journal*.
- [2] Bagdasaryan, E., Veit, A., Hua, Y., Estrin, D., and Shmatikov, V. (2020). How to backdoor federated learning. In *International conference on artificial intelligence and statistics*, pages 2938–2948. PMLR.
- [3] Barni, M., Kallas, K., and Tondi, B. (2019). A new backdoor attack in cnns by training set corruption without label poisoning. In *2019 IEEE International Conference on Image Processing (ICIP)*, pages 101–105. IEEE.
- [4] Baruch, G., Baruch, M., and Goldberg, Y. (2019). A little is enough: Circumventing defenses for distributed learning. *Advances in Neural Information Processing Systems*, 32.
- [5] Bhagoji, A. N., Chakraborty, S., Mittal, P., and Calo, S. (2019). Analyzing federated learning through an adversarial lens. In *International Conference on Machine Learning*, pages 634–643. PMLR.
- [6] Chellapandi, V. P., Yuan, L., Žak, S. H., and Wang, Z. (2023). A survey of federated learning for connected and automated vehicles. In *2023 IEEE 26th International Conference on Intelligent Transportation Systems (ITSC)*, pages 2485–2492. IEEE.
- [7] Chen, X., Liu, C., Li, B., Lu, K., and Song, D. (2017). Targeted backdoor attacks on deep learning systems using data poisoning. *arXiv preprint arXiv:1712.05526*.
- [8] Chen, Z., Badrinarayanan, V., Lee, C.-Y., and Rabinovich, A. (2018). Gradnorm: Gradient normalization for adaptive loss balancing in deep multitask networks. In *International conference on machine learning*, pages 794–803. PMLR.
- [9] Feng, Y., Ma, B., Zhang, J., Zhao, S., Xia, Y., and Tao, D. (2022). Fiba: Frequency-injection based backdoor attack in medical image analysis. In *Proceedings of the IEEE/CVF Conference on Computer Vision and Pattern Recognition*, pages 20876–20885.
- [10] Fung, C., Yoon, C. J., and Beschastnikh, I. (2018). Mitigating sybils in federated learning poisoning. *arXiv preprint arXiv:1808.04866*.
- [11] Geyer, R. C., Klein, T., and Nabi, M. (2017). Differentially private federated learning: A client level perspective. *arXiv preprint arXiv:1712.07557*.
- [12] Gong, X., Chen, Y., Wang, Q., and Kong, W. (2022). Backdoor attacks and defenses in federated learning: State-of-the-art, taxonomy, and future directions. *IEEE Wireless Communications*, 30(2):114–121.

- [13] Gu, T., Dolan-Gavitt, B., and Garg, S. (2017). Badnets: Identifying vulnerabilities in the machine learning model supply chain. *arXiv preprint arXiv:1708.06733*.
- [14] He, K., Zhang, X., Ren, S., and Sun, J. (2016). Deep residual learning for image recognition. In *Proceedings of the IEEE conference on computer vision and pattern recognition*, pages 770–778.
- [15] Hessel, M., Modayil, J., Van Hasselt, H., Schaul, T., Ostrovski, G., Dabney, W., Horgan, D., Piot, B., Azar, M., and Silver, D. (2018). Rainbow: Combining improvements in deep reinforcement learning. In *Proceedings of the AAAI conference on artificial intelligence*, volume 32.
- [16] Hou, L., Hua, Z., Li, Y., and Zhang, L. Y. (2022). M-to-n backdoor paradigm: A stealthy and fuzzy attack to deep learning models. *arXiv preprint arXiv:2211.01875*.
- [17] Jiang, W., Li, H., Xu, G., and Zhang, T. (2023). Color backdoor: A robust poisoning attack in color space. In *Proceedings of the IEEE/CVF Conference on Computer Vision and Pattern Recognition*, pages 8133–8142.
- [18] Kendall, A., Gal, Y., and Cipolla, R. (2018). Multi-task learning using uncertainty to weigh losses for scene geometry and semantics. In *Proceedings of the IEEE conference on computer vision and pattern recognition*, pages 7482–7491.
- [19] Konecny, J., McMahan, H. B., Yu, F. X., Richtárik, P., Suresh, A. T., and Bacon, D. (2016). Federated learning: Strategies for improving communication efficiency. *arXiv preprint arXiv:1610.05492*, 8.
- [20] Krizhevsky, A., Hinton, G., et al. (2009). Learning multiple layers of features from tiny images.
- [21] Kwon, H. (2022). Multi-model selective backdoor attack with different trigger positions. *IEICE TRANSACTIONS on Information and Systems*, 105(1):170–174.
- [22] Kwon, H., Roh, J., Yoon, H., and Park, K.-W. (2020a). Targetnet backdoor: attack on deep neural network with use of different triggers. In *Proceedings of the 2020 5th International Conference on Intelligent Information Technology*, pages 140–145.
- [23] Kwon, H., Yoon, H., and Park, K.-W. (2020b). Multi-targeted backdoor: Identifying backdoor attack for multiple deep neural networks. *IEICE TRANSACTIONS on Information and Systems*, 103(4):883–887.
- [24] Lesort, T. (2020). Continual learning: Tackling catastrophic forgetting in deep neural networks with replay processes. *arXiv preprint arXiv:2007.00487*.
- [25] Li, S., Ngai, E. C.-H., and Voigt, T. (2023). An experimental study of byzantine-robust aggregation schemes in federated learning. *IEEE Transactions on Big Data*.
- [26] Li, Y. (2023). Poisoning-based backdoor attacks in computer vision. In *Proceedings of the AAAI Conference on Artificial Intelligence*, volume 37, pages 16121–16122.
- [27] Liu, S., Johns, E., and Davison, A. J. (2019). End-to-end multi-task learning with attention. In *Proceedings of the IEEE/CVF conference on computer vision and pattern recognition*, pages 1871–1880.
- [28] Liu, T., Wang, Z., He, H., Shi, W., Lin, L., An, R., and Li, C. (2023). Efficient and secure federated learning for financial applications. *Applied Sciences*, 13(10):5877.
- [29] Liu, T., Zhang, Y., Feng, Z., Yang, Z., Xu, C., Man, D., and Yang, W. (2024). Beyond traditional threats: A persistent backdoor attack on federated learning. In *Proceedings of the AAAI Conference on Artificial Intelligence*, volume 38, pages 21359–21367.
- [30] Mamba Kabala, D., Hafiane, A., Bobelin, L., and Canals, R. (2023). Image-based crop disease detection with federated learning. *Scientific Reports*, 13(1):19220.
- [31] McMahan, B., Moore, E., Ramage, D., Hampson, S., and y Arcas, B. A. (2017a). Communication-efficient learning of deep networks from decentralized data. In *Artificial intelligence and statistics*, pages 1273–1282. PMLR.
- [32] McMahan, H. B., Ramage, D., Talwar, K., and Zhang, L. (2017b). Learning differentially private recurrent language models. *arXiv preprint arXiv:1710.06963*.
- [33] Mnih, V., Kavukcuoglu, K., Silver, D., Rusu, A. A., Veness, J., Bellemare, M. G., Graves, A., Riedmiller, M., Fidjeland, A. K., Ostrovski, G., et al. (2015). Human-level control through deep reinforcement learning. *nature*, 518(7540):529–533.

- [34] Nguyen, T. D., Nguyen, T., Le Nguyen, P., Pham, H. H., Doan, K. D., and Wong, K.-S. (2024). Backdoor attacks and defenses in federated learning: Survey, challenges and future research directions. *Engineering Applications of Artificial Intelligence*, 127:107166.
- [35] Paszke, A., Gross, S., Massa, F., Lerer, A., Bradbury, J., Chanan, G., Killeen, T., Lin, Z., Gimelshein, N., Antiga, L., et al. (2019). Pytorch: An imperative style, high-performance deep learning library. *Advances in neural information processing systems*, 32.
- [36] Salem, A., Wen, R., Backes, M., Ma, S., and Zhang, Y. (2022). Dynamic backdoor attacks against machine learning models. In *2022 IEEE 7th European Symposium on Security and Privacy (EuroS&P)*, pages 703–718. IEEE.
- [37] Schaul, T., Quan, J., Antonoglou, I., and Silver, D. (2015). Prioritized experience replay. *arXiv preprint arXiv:1511.05952*.
- [38] Shafahi, A., Huang, W. R., Najibi, M., Suci, O., Studer, C., Dumitras, T., and Goldstein, T. (2018). Poison frogs! targeted clean-label poisoning attacks on neural networks. *Advances in neural information processing systems*, 31.
- [39] Shannon, C. E. (1949). Communication theory of secrecy systems. *The Bell system technical journal*, 28(4):656–715.
- [40] Shejwalkar, V., Houmansadr, A., Kairouz, P., and Ramage, D. (2022). Back to the drawing board: A critical evaluation of poisoning attacks on production federated learning. In *2022 IEEE Symposium on Security and Privacy (SP)*, pages 1354–1371. IEEE.
- [41] Sheller, M. J., Edwards, B., Reina, G. A., Martin, J., Pati, S., Kotrotsou, A., Milchenko, M., Xu, W., Marcus, D., Colen, R. R., et al. (2020). Federated learning in medicine: facilitating multi-institutional collaborations without sharing patient data. *Scientific reports*, 10(1):12598.
- [42] So, J., Ali, R. E., Güler, B., Jiao, J., and Avestimehr, A. S. (2023). Securing secure aggregation: Mitigating multi-round privacy leakage in federated learning. In *Proceedings of the AAAI Conference on Artificial Intelligence*, volume 37, pages 9864–9873.
- [43] Stallkamp, J., Schlipsing, M., Salmen, J., and Igel, C. (2011). The german traffic sign recognition benchmark: a multi-class classification competition. In *The 2011 international joint conference on neural networks*, pages 1453–1460. IEEE.
- [44] Tolpegin, V., Truex, S., Gursoy, M. E., and Liu, L. (2020). Data poisoning attacks against federated learning systems. In *Computer Security—ESORICS 2020: 25th European Symposium on Research in Computer Security, ESORICS 2020, Guildford, UK, September 14–18, 2020, Proceedings, Part I 25*, pages 480–501. Springer.
- [45] Wang, H., Sreenivasan, K., Rajput, S., Vishwakarma, H., Agarwal, S., Sohn, J.-y., Lee, K., and Papailiopoulos, D. (2020). Attack of the tails: Yes, you really can backdoor federated learning. *Advances in Neural Information Processing Systems*, 33:16070–16084.
- [46] Wang, R., Zhou, G., Gao, M., and Xiao, Y. (2024). Dual model replacement: invisible multi-target backdoor attack based on federal learning. *arXiv preprint arXiv:2404.13946*.
- [47] Wang, T., Yao, Y., Xu, F., An, S., Tong, H., and Wang, T. (2022a). An invisible black-box backdoor attack through frequency domain. In *European Conference on Computer Vision*, pages 396–413. Springer.
- [48] Wang, Y., Zhao, M., Li, S., Yuan, X., and Ni, W. (2022b). Dispersed pixel perturbation-based imperceptible backdoor trigger for image classifier models. *IEEE Transactions on Information Forensics and Security*, 17:3091–3106.
- [49] Wang, Z. and Bovik, A. C. (2002). A universal image quality index. *IEEE signal processing letters*, 9(3):81–84.
- [50] Wang, Z., Bovik, A. C., Sheikh, H. R., and Simoncelli, E. P. (2004). Image quality assessment: from error visibility to structural similarity. *IEEE transactions on image processing*, 13(4):600–612.
- [51] Wu, C., Yang, X., Zhu, S., and Mitra, P. (2020). Mitigating backdoor attacks in federated learning. *arXiv preprint arXiv:2011.01767*.
- [52] Wu, C., Zhu, S., and Mitra, P. (2022). Federated unlearning with knowledge distillation. *arXiv preprint arXiv:2201.09441*.

- [53] Xie, C., Huang, K., Chen, P.-Y., and Li, B. (2019). Dba: Distributed backdoor attacks against federated learning. In *International conference on learning representations*.
- [54] Xue, M., He, C., Wang, J., and Liu, W. (2020). One-to-n & n-to-one: Two advanced backdoor attacks against deep learning models. *IEEE Transactions on Dependable and Secure Computing*, 19(3):1562–1578.
- [55] Xue, M., Ni, S., Wu, Y., Zhang, Y., Wang, J., and Liu, W. (2022). Imperceptible and multi-channel backdoor attack against deep neural networks. *arXiv preprint arXiv:2201.13164*.
- [56] Yang, Q., Liu, Y., Chen, T., and Tong, Y. (2019). Federated machine learning: Concept and applications. *ACM Transactions on Intelligent Systems and Technology (TIST)*, 10(2):1–19.
- [57] Yu, Y., Wang, Y., Yang, W., Lu, S., Tan, Y.-P., and Kot, A. C. (2023). Backdoor attacks against deep image compression via adaptive frequency trigger. In *Proceedings of the IEEE/CVF Conference on Computer Vision and Pattern Recognition*, pages 12250–12259.
- [58] Zhang, R., Isola, P., Efros, A. A., Shechtman, E., and Wang, O. (2018). The unreasonable effectiveness of deep features as a perceptual metric. In *Proceedings of the IEEE conference on computer vision and pattern recognition*, pages 586–595.
- [59] Zhang, Z., Cao, X., Jia, J., and Gong, N. Z. (2022a). Fldetector: Defending federated learning against model poisoning attacks via detecting malicious clients. In *Proceedings of the 28th ACM SIGKDD Conference on Knowledge Discovery and Data Mining*, pages 2545–2555.
- [60] Zhang, Z., Panda, A., Song, L., Yang, Y., Mahoney, M., Mittal, P., Kannan, R., and Gonzalez, J. (2022b). Neurotoxin: Durable backdoors in federated learning. In *International Conference on Machine Learning*, pages 26429–26446. PMLR.

A Details of the Experiment in Fig. 1

In the initial phase of our investigation, extensive explorations were conducted to assess the efficacy of existing backdoor attack methods in distributed multi-target environments. Our findings indicated a significant degradation in performance, particularly in sustaining multiple persistent backdoors. For instance, our experiments on the GTSRB dataset involved three attackers (illustrated in Fig. 1), each managing a client. These clients independently activated distinct backdoors using a uniform trigger at varying levels of transparency, without the integration of a backdoor replay mechanism. The results demonstrated a consistent pattern: the introduction of a new backdoor consistently neutralized the effectiveness of its predecessors, underscoring the inability of the global model to maintain multiple backdoors simultaneously.

B Trigger Strategy Details & More Attackers

In this section, we outline the backdoor strategies employed in Distributed Multi-target Backdoor Attacks (DMBA) when implemented with three and six attackers. We specify the target labels, channels, and frequency blocks utilized by each attacker, as detailed in Tab. 5. Furthermore, Tab. 6 presents the attack performance for DMBA with six attackers, where the average Attack Success Rate (ASR) exceeds 90% across 30 attack rounds. These results underscore DMBA’s capability to maintain high efficiency and persistence in distributed multi-target scenarios.

CIFAR-100		
Targets	n=3	n=6
1	#10	#10
2	#47	#47
Labels 3	#59	#59
4	-	#61
5	-	#78
6	-	#90
1	R:[15,15]-[17,17]	R:[15,15]-[17,17]
2	G:[20,20]-[22,22]	R:[25,25]-[27,27]
Blocks 3	B:[25,25]-[27,27]	G:[15,15]-[17,17]
4	-	G:[25,25]-[27,27]
5	-	B:[15,15]-[17,17]
6	-	B:[25,25]-[27,27]

Datasets	CIFAR-10	CIFAR-100	GTSRB
ACC	75.73%	45.66%	94.30%
1	99.80%	97.21%	96.46%
2	99.41%	99.64%	99.89%
ASR 3	99.68%	96.52%	94.12%
4	99.70%	99.65%	99.69%
5	99.07%	87.98%	98.97%
6	99.76%	88.40%	98.93%
1	99.82%	61.28%	78.58%
2	99.83%	91.64%	99.98%
ASR-30 3	99.04%	86.98%	88.69%
4	99.80%	72.02%	98.08%
5	99.68%	89.75%	98.74%
6	99.84%	90.66%	91.15%

C Deriving the Components of the Attacker’s Training Data

Here, we consider a scenario with three attackers (n=3). For Attacker-1, we calculate the total data D_{b_1} involved in training. This dataset includes local data D_{local} and data from the replay pool $Pool_{br}$. From $Pool_{br}$, we remove the first type of backdoor samples while retaining the remaining two types for replay. The local data D_{local} comprises backdoor samples D_{poi_1} crafted by the attacker and clean samples. Consequently, D_{b_1} integrates these three types of backdoor samples and clean samples. The formula to derive D_{b_1} is presented below:

$$\begin{aligned}
D_{b_1} &= D_{local} + Pool_{br} \setminus D_{br_1} \\
&= D_{local} + D_{br_2} + D_{br_3} \\
&= D_{poi_1} + D_{cln} + D_{br_2} + D_{br_3} \\
&= D_{poi_1} + D_{poi_2} + D_{poi_3} + D_{cln}
\end{aligned}$$

Similarly for D_{b_2} and D_{b_3} , so we get Eq. 3.

D Attack Performance Comparison of Replay with Pool vs. Direct Replay

As detailed in Section 4.1, we evaluated the attack performance of Distributed Multi-target Backdoor Attacks (DMBA) using two replay methods. Our analysis, as presented in Tab. 7, reveals that both methods exhibit comparable performance in most scenarios.

Table 7: Attack performance comparison of replay with pool vs. direct replay.

Datasets	CIFAR-10		CIFAR-100		GTSRB	
	Direct Replay	Replay with Pool	Direct Replay	Replay with Pool	Direct Replay	Replay with Pool
ACC	73.30%	72.80%	52.63%	52.93%	98.13%	98.07%
Att1	96.91%	98.92%	91.19%	96.99%	98.72%	93.73%
ASR Att2	94.49%	99.08%	95.80%	94.99%	99.83%	99.80%
Att3	99.28%	92.68%	92.25%	95.25%	99.30%	95.88%
Att1	78.42%	91.81%	69.07%	83.07%	96.79%	81.48%
ASR-30 Att2	89.34%	95.20%	87.96%	69.90%	99.67%	99.82%
Att3	97.01%	69.04%	58.71%	80.78%	99.25%	92.34%

E Assessment of Invisibility on Each Dataset

This section presents the results of the invisibility evaluation conducted on three datasets, detailed in Tab. 8. The findings align with those discussed in Section 4.3, indicating that the triggers employed in Distributed Multi-target Backdoor Attacks (DMBA) generally exhibit superior invisibility across most scenarios.

Table 8: Invisibility assessment of different attacks on CIFAR-10, CIFAR-100 and GTSRB.

Datasets	CIFAR-10				CIFAR-100				GTSRB				
Methods	DMBA	BadNets-t	DMM	TargetNet-l	DMBA	BadNets-t	DMM	TargetNet-l	DMBA	BadNets-t	DMM	TargetNet-l	
SSIM	Att1	0.98446	0.95843	0.95418	0.97250	0.98428	0.95852	0.95216	0.97392	0.97694	0.93283	0.91078	0.96460
	Att2	0.98396	0.93318	0.95265	0.97164	0.98420	0.93533	0.95073	0.97217	0.97697	0.90495	0.91425	0.96187
	Att3	0.98328	0.91964	0.95073	0.97262	0.98343	0.92287	0.94774	0.97401	0.97792	0.89517	0.91729	0.96463
PSNR	Att1	81.5933	70.8548	77.6580	70.8916	81.5933	71.4822	77.7176	72.1541	81.5933	68.9160	77.5953	68.2612
	Att2	81.5933	66.8446	77.6456	69.1680	81.5933	67.7334	77.6902	70.2865	81.5933	64.1737	77.6407	66.2608
	Att3	81.5933	64.8733	77.6860	70.8790	81.5933	65.8307	77.7560	72.1614	81.5933	62.1481	77.5856	67.8524
LPIPS	Att1	0.0283	0.0784	0.0586	0.0675	0.0266	0.0746	0.0594	0.0630	0.05052	0.1174	0.12473	0.0953
	Att2	0.0445	0.1251	0.0950	0.0668	0.0489	0.1176	0.0918	0.0638	0.08314	0.1721	0.19052	0.0867
	Att3	0.0074	0.1553	0.0321	0.0684	0.0116	0.1460	0.0320	0.0631	0.02482	0.2018	0.06216	0.0915

F More Parametric Sensitivity Analyses

This section provides a detailed analysis of how various factors influence the performance of Distributed Multi-target Backdoor Attacks (DMBA). These factors include block start position, perturbation amplitude, the ratio of poisoning to backdoor replay, block size, the interval between injection rounds, and the selection of target classes.

F.1 Effect of Frequency Block Position

This section examines the impact of the initial position of the frequency blocks on the attack and stealth performance of Distributed Multi-target Backdoor Attacks (DMBA) across three datasets. Tab. 9 illustrates that DMBA achieves optimal attack efficiency and persistence with the initial positions of frequency blocks set at '15/20/25', a strategy detailed in Section 4.5. Additionally, Tab. 10 indicates that targeting the high-frequency region for perturbation enhances stealthiness. This is because the low-frequency region carries the primary information of the image, and perturbing it is more likely to result in noticeable visual anomalies.

Table 9: Effect of frequency block position on attack performance.

Datasets	CIFAR-10			CIFAR-100			GTSRB			
Frequency Block Position	15/20/25	15/15/15	5/15/25	15/20/25	15/15/15	5/15/25	15/20/25	15/15/15	5/15/25	
ACC	73.30%	72.66%	73.66%	52.63%	50.33%	52.38%	98.13%	97.05%	97.72%	
ASR	Att1	96.91%	76.18%	78.86%	91.19%	89.58%	8.41%	98.72%	99.92%	90.18%
	Att2	94.49%	91.10%	97.79%	95.80%	96.34%	94.16%	99.83%	99.36%	99.66%
	Att3	99.28%	97.83%	98.07%	92.25%	94.48%	93.63%	99.31%	88.58%	15.20%
ASR-30	Att1	78.42%	73.27%	35.49%	69.07%	76.59%	0.39%	96.79%	98.63%	83.18%
	Att2	89.34%	94.39%	96.41%	87.96%	81.34%	75.33%	99.67%	98.99%	99.48%
	Att3	97.01%	78.91%	93.60%	58.71%	64.41%	79.73%	99.25%	60.82%	0.86%

Table 10: Effect of frequency block position on stealth performance.

Datasets	CIFAR-10					CIFAR-100					GTSRB					
Location	5	10	15	20	25	5	10	15	20	25	5	10	15	20	25	
SSIM	Att1	0.98507	0.98454	0.98446	0.98447	0.98435	0.98487	0.98436	0.98428	0.98429	0.98418	0.97780	0.97708	0.97694	0.97697	0.97683
	Att2	0.98460	0.98403	0.98395	0.98396	0.98385	0.98483	0.98428	0.98420	0.98422	0.98410	0.97772	0.97711	0.97697	0.97700	0.97685
	Att3	0.98403	0.98347	0.98338	0.98340	0.98328	0.98403	0.98351	0.98343	0.98344	0.98333	0.97874	0.97805	0.97792	0.97795	0.97780
PSNR	Att1	81.5933	81.5933	81.5933	81.5933	81.5933	81.5933	81.5933	81.5933	81.5933	81.5933	81.5933	81.5933	81.5933	81.5933	81.5933
	Att2	81.5933	81.5933	81.5933	81.5933	81.5933	81.5933	81.5933	81.5933	81.5933	81.5933	81.5933	81.5933	81.5933	81.5933	81.5933
	Att3	81.5933	81.5933	81.5933	81.5933	81.5933	81.5933	81.5933	81.5933	81.5933	81.5933	81.5933	81.5933	81.5933	81.5933	81.5933
LPIPS	Att1	0.0333	0.0257	0.0283	0.0248	0.0067	0.0309	0.0240	0.0266	0.0234	0.0062	0.05020	0.04606	0.05052	0.04630	0.01487
	Att2	0.0416	0.0457	0.0515	0.0445	0.0107	0.0380	0.0431	0.0489	0.0424	0.0099	0.06985	0.07629	0.08314	0.07518	0.02243
	Att3	0.0212	0.0135	0.0125	0.0170	0.0074	0.0194	0.0122	0.0116	0.0159	0.0069	0.03342	0.02569	0.02482	0.03365	0.01630

F.2 Effect of Perturbation Magnitude

This section analyzes the impact of perturbation magnitude on the attack and stealth performance of backdoor attacks across three datasets. According to Tab. 11 and 12, increasing the perturbation amplitude enhances the Attack Success Rate (ASR) and persistence of the backdoor. However, this comes at the cost of reduced invisibility. Thus, selecting the appropriate perturbation amplitude requires careful consideration to balance effectiveness and stealth.

Table 11: Effect of perturbation magnitude on attack performance.

Datasets	CIFAR-10					CIFAR-100					GTSRB					
Perturbation Magnitude	80	90	100	110	120	80	90	100	110	120	80	90	100	110	120	
ACC	72.20%	72.32%	73.30%	73.12%	73.57%	52.47%	51.97%	52.63%	52.75%	52.26%	97.14%	97.84%	98.13%	98.05%	98.17%	
ASR	Att1	94.23%	98.34%	96.91%	98.31%	89.44%	80.88%	91.29%	91.19%	95.67%	93.75%	97.76%	95.47%	98.72%	97.81%	94.21%
	Att2	96.60%	94.99%	94.49%	95.90%	92.38%	91.08%	91.27%	95.80%	90.61%	95.21%	99.79%	99.95%	99.83%	99.75%	99.85%
	Att3	98.63%	98.80%	99.28%	99.52%	98.36%	23.65%	89.02%	92.25%	93.10%	93.96%	99.84%	99.44%	99.31%	99.44%	99.92%
ASR-30	Att1	73.53%	75.38%	78.42%	86.94%	63.80%	65.72%	70.26%	69.07%	80.56%	83.95%	89.13%	82.89%	96.79%	97.31%	94.52%
	Att2	89.08%	87.39%	89.34%	81.36%	92.02%	75.82%	82.59%	87.96%	82.86%	91.90%	85.50%	99.53%	99.67%	98.78%	97.69%
	Att3	95.33%	91.80%	97.01%	93.86%	97.42%	19.77%	76.28%	58.71%	84.08%	89.11%	99.91%	98.91%	99.25%	98.93%	99.83%

Table 12: Effect of perturbation magnitude on stealth performance.

Datasets	CIFAR-10					CIFAR-100					GTSRB					
Perturbation Magnitude	80	90	100	110	120	80	90	100	110	120	80	90	100	110	120	
SSIM	Att1	0.98886	0.98668	0.98446	0.98221	0.97994	0.98877	0.98655	0.98428	0.98197	0.97965	0.98313	0.98005	0.97694	0.97384	0.97076
	Att2	0.98847	0.98623	0.98395	0.98164	0.97932	0.98872	0.98649	0.98420	0.98188	0.97954	0.98308	0.98003	0.97697	0.97393	0.97091
	Att3	0.98802	0.98572	0.98338	0.98101	0.97864	0.98813	0.98580	0.98343	0.98102	0.97859	0.98378	0.98086	0.97792	0.97500	0.97209
PSNR	Att1	83.5315	82.5085	81.5933	80.7655	80.0097	83.5315	82.5085	81.5933	80.7655	80.0098	83.5315	82.5085	81.5933	80.7655	80.0097
	Att2	83.5315	82.5085	81.5933	80.7655	80.0097	83.5315	82.5085	81.5933	80.7655	80.0098	83.5315	82.5085	81.5933	80.7655	80.0097
	Att3	83.5315	82.5085	81.5933	80.7655	80.0097	83.5315	82.5085	81.5933	80.7655	80.0098	83.5315	82.5085	81.5933	80.7655	80.0097
LPIPS	Att1	0.0193	0.0237	0.0283	0.0331	0.0381	0.0180	0.0222	0.0266	0.0312	0.0360	0.0363	0.0434	0.0505	0.0577	0.0649
	Att2	0.0366	0.0439	0.0515	0.0592	0.0670	0.0346	0.0417	0.0489	0.0563	0.0638	0.0624	0.0728	0.0831	0.0932	0.1032
	Att3	0.0081	0.0102	0.0125	0.0150	0.0175	0.0075	0.0095	0.0116	0.0139	0.0163	0.0169	0.0208	0.02482	0.0290	0.0333

F.3 Impact of Poisoning Ratio and Backdoor Replay Ratio

This section explores the influence of the poisoning ratio and backdoor replay ratio on the performance of backdoor attacks across three datasets. Tab. 13 demonstrates that higher poisoning ratios and backdoor replay ratios significantly improve the effectiveness of the corresponding backdoors.

Table 13: Impact of poisoning ratio and backdoor replay ratio on attack performance.

Datasets	CIFAR-10					CIFAR-100					GTSRB					
Ratio	1/1/4	2/2/4	3/3/8	4/4/10	5/5/12	1/1/4	2/2/4	3/3/8	4/4/10	5/5/12	1/1/4	2/2/4	3/3/8	4/4/10	5/5/12	
ACC	74.31%	72.77%	73.30%	73.02%	73.42%	52.99%	53.19%	52.63%	51.96%	48.31%	98.75%	98.06%	98.13%	97.23%	96.76%	
ASR	Att1	97.04%	91.80%	96.91%	96.71%	98.69%	22.02%	93.20%	91.19%	94.62%	96.46%	91.39%	77.93%	98.72%	98.55%	99.30%
	Att2	92.83%	91.29%	94.49%	96.70%	95.16%	85.84%	81.06%	95.80%	94.25%	98.12%	99.35%	97.49%	99.83%	99.74%	99.95%
	Att3	13.74%	95.72%	99.28%	99.91%	99.18%	3.16%	61.70%	92.25%	94.38%	96.48%	91.17%	7.041%	99.31%	95.25%	100%
ASR-30	Att1	80.03%	61.54%	78.42%	91.09%	91.60%	17.63%	78.28%	69.07%	85.28%	83.22%	78.15%	79.12%	96.79%	81.19%	99.02%
	Att2	91.41%	77.59%	89.34%	83.77%	85.76%	76.86%	52.43%	87.96%	87.52%	92.88%	98.58%	88.85%	99.67%	96.85%	99.87%
	Att3	6.01%	86.89%	97.01%	96.74%	93.32%	1.38%	69.47%	58.71%	85.16%	88.18%	70.39%	0.82%	99.25%	79.27%	99.87%

F.4 Effect of Frequency Block Size

We hypothesized that the size of the frequency block might influence the attack performance of Distributed Multi-target Backdoor Attacks (DMBA). To test this, we experimented with frequency blocks sized 1*1, 2*2, and 3*3 for perturbation. The experimental results, detailed in Tab. 14, indicate that perturbing larger frequency blocks generally enhances the attack performance of DMBA.

Table 14: Effect of frequency block size on attack performance.

Datasets	CIFAR-10			CIFAR-100			GTSRB			
Block Size	1*1	2*2	3*3	1*1	2*2	3*3	1*1	2*2	3*3	
ACC	73.27%	72.79%	73.30%	52.89%	52.35%	52.63%	98.33%	99.10%	98.13%	
ASR	Att1	91.49%	87.67%	96.91%	3.57%	0.33%	91.19%	99.66%	96.09%	98.72%
	Att2	97.82%	99.03%	94.49%	34.49%	99.1%	95.80%	99.69%	99.86%	99.82%
	Att3	98.88%	96.43%	99.28%	2.11%	3.32%	92.25%	97.22%	99.88%	99.31%
ASR-30	Att1	25.71%	92.22%	78.42%	0.12%	0.32%	69.07%	98.01%	94.33%	96.79%
	Att2	30.68%	77.30%	89.34%	0.11%	99.77%	87.96%	99.85%	83.55%	99.67%
	Att3	36.46%	74.51%	97.01%	0.14%	2.56%	58.71%	85.90%	94.30%	99.25%

F.5 Effect of Poison Injection Round Interval

We hypothesized that the interval between poison injection rounds could impact the performance of Distributed Multi-target Backdoor Attacks (DMBA). To investigate, we set the poison injection intervals at fixed rounds of 2, 5, 10, as well as at randomly varying intervals. The experimental outcomes, presented in Tab. 15, suggest that extending the interval between rounds tends to enhance DMBA’s attack performance. This improvement likely occurs because shorter intervals can cause significant gradient conflicts among different backdoors, undermining the effectiveness of some backdoors.

Table 15: Effect of poison injection round interval on attack performance.

Datasets	CIFAR-10				CIFAR-100				GTSRB				
Injection Interval	2	5	10	Random	2	5	10	Random	2	5	10	Random	
ACC	73.30%	74.87%	75.58%	72.20%	52.63%	53.72%	56.83%	53.35%	98.13%	98.36%	98.05%	99.07%	
ASR	Att1	96.91%	97.91%	99.90%	98.72%	91.19%	93.20%	98.32%	94.62%	98.72%	99.61%	99.80%	99.53%
	Att2	94.49%	99.01%	98.16%	99.09%	95.80%	90.60%	97.48%	96.41%	99.83%	99.56%	99.97%	99.91%
	Att3	99.28%	99.58%	99.89%	99.81%	92.25%	3.44%	89.92%	95.32%	99.31%	98.89%	99.97%	99.60%
ASR-30	Att1	78.42%	74.86%	98.73%	93.79%	69.07%	69.07%	90.09%	82.98%	96.79%	94.32%	98.79%	96.54%
	Att2	89.34%	89.34%	86.48%	94.47%	87.96%	87.96%	83.85%	83.77%	99.69%	97.42%	100%	99.84%
	Att3	97.01%	94.09%	93.90%	95.18%	58.71%	7.63%	75.33%	91.28%	99.25%	99.49%	99.20%	99.85%

F.6 Impact of Target Class Choice

We theorized that the choice of target class might influence the attack performance of Distributed Multi-target Backdoor Attacks (DMBA). To explore this, we conducted experiments using various target classes, with the results displayed in Tab. 16. Interestingly, our findings indicate that the choice of target class does not significantly impact the attack performance of DMBA.

Table 16: Impact of target class choice on attack performance.

Datasets	CIFAR-10			CIFAR-100			GTSRB			
Target Labels	[0,4,6]	[1,3,9]	[2,7,8]	[15-20-25]	[4,57,89]	[26,34,90]	[0,20,29]	[3,17,25]	[10,24,40]	
ACC	73.30%	68.78%	70.97%	52.63%	52.61%	53.64%	98.13%	97.27%	98.11%	
ASR	Att1	96.91%	95.80%	97.01%	91.19%	97.32%	95.70%	98.72%	96.01%	96.09%
	Att2	94.49%	97.29%	99.39%	95.80%	96.84%	96.24%	99.83%	98.54%	99.86%
	Att3	99.28%	94.91%	95.13%	92.25%	93.21%	93.37%	99.31%	96.44%	99.88%
ASR-30	Att1	78.42%	96.49%	94.09%	69.07%	84.89%	77.93%	96.79%	89.28%	94.33%
	Att2	89.34%	81.14%	88.01%	87.96%	72.14%	86.28%	99.67%	97.73%	83.55%
	Att3	97.01%	96.99%	85.46%	58.71%	73.00%	73.00%	99.25%	92.91%	94.30%

G Robustness Validation on Each Dataset

In this section, we present the robustness validation of Distributed Multi-target Backdoor Attacks (DMBA) across three datasets, with the experimental results detailed in Tab. 17. Our analysis reveals that two advanced In-AD defense methods fail to fully neutralize the threat posed by DMBA, thereby affirming its substantial robustness.

Table 17: Robustness validation of DMBA on CIFAR-10, CIFAR-100 and GTSRB.

Datasets	CIFAR-10			CIFAR-100			GTSRB			
Defense Methods	No Defense	ClippedClustering	DP-FedAvg	No Defense	ClippedClustering	DP-FedAvg	No Defense	ClippedClustering	DP-FedAvg	
ACC	73.30	74.76	78.30	52.63	59.36	71.03	98.13	98.62	99.84	
ASR	Att1	96.91	66.02	51.94	91.19	90.16	54.19	96.91	17.83	99.52
	Att2	94.49	60.09	46.97	95.80	79.67	3.61	94.49	23.35	0.27
	Att3	99.28	94.12	66.18	92.25	66.85	36.26	99.28	80.00	30.37
ASR-30	Att1	78.42	34.03	57.03	69.07	71.55	60.59	96.79	2.16	99.52
	Att2	89.34	35.79	61.28	87.96	69.32	43.79	99.67	9.20	2.60
	Att3	97.01	81.78	66.86	58.71	34.73	50.99	99.25	71.99	14.31